I-V ANALYSIS OF IRRADIATED GALLIUM ARSENIDE SOLAR CELLS[*]

A. Meulenberg
COMSAT Laboratories
Clarksburg, Maryland

and

R. H. Maurer and J. D. Kinnison
The Johns Hopkins University Applied Physics Laboratory
Laurel, Maryland

While a spacecraft designer may only be interested in end-of-life (EOL) solar cell output power, analysis of the full I-V characteristics of unirradiated and irradiated cells can benefit both the solar cell designer and manufacturer, as well as those responsible for determining solar cell acceptance criteria. COMSAT Laboratories has used a computer program to analyze the illuminated I-V characteristics of four sets of gallium arsenide (GaAs) solar cells irradiated by the Johns Hopkins University Applied Physics Laboratory (APL) with 1-MeV electrons and 10-MeV protons.

The illuminated I-V characteristic provides the values (under operating conditions) for series resistance (R_s), minority carrier lifetime, internal electric fields, and other cell parameters which may depend on photo-generated carrier concentrations. A multi-regression fit of these data is made to the following equation:

$$I = I_{ro}\left[e^{q(V-IR_S)/2kT} - 1\right] + I_{do}\left[e^{q(V-IR_S)/kT} - 1\right] - (V - IR_S)/(R_{sh}) - I_L \tag{1}$$

where

I	=	output current
I_{ro} and I_{do}	=	coefficients of the junction recombination and bulk dark currents, respectively
I_L	=	photo-generated short-circuit current
V	=	cell voltage ($V - IR_s = V_j$, the junction voltage)
R_{sh}	=	junction shunt resistance.

The short-circuit current, I_L, is subtracted and the data are fitted (with R_s being stepped to obtain the best correlation) to determine values for R_s, R_{sh}, I_{do}, and I_{ro}. In the simplest analysis, these are all constants. The two currents separate the equation into contributions from bulk regions, J_d, and junction regions, J_r. (Current densities are used to remove area effects.) More detailed analysis (ref. 1) employs the full Sah-Noyce-Schockley formulation for J_{ro}, which allows determination of non-midgap defect levels, and band gap narrowing due to the Franz-Keldysh effect.

I-V analysis has been used for silicon solar cells (ref. 2) to measure the effectiveness of the following:

- p^+ back contact treatments.
- Treatments to reduce surface recombination.
- Dot contacts vs grids.
- Altered junction profiles.
- Gettering to increase diffusion lengths.
- Many other processing changes.

This method has also been used for analyzing silicon solar cells to determine the following:

- Band gap narrowing from heavy doping (ref. 1).
- Band gap narrowing from intense electric fields (ref. 1).
- The presence of A-centers in the junction, resulting from oxygen diffusion during n^+ layer formation (unpublished data).
- The presence and nature of junction leakage paths caused by heavy-ion bombardment (ref. 3).
- The best approach for improving beginning-of-life (BOL) or EOL performance (ref. 4).

Since I-V analysis had been successfully applied to silicon cells (ref. 2), it was thought that it might be equally beneficial when used for GaAs cells, such as those irradiated by APL (ref. 5, 6). The analysis of representative unirradiated GaAs cells in this experiment indicates that the junction recombination current density (J_r) dominates the contributions to the dark current. At 0.82 V, which is the voltage at maximum power, the bulk dark-current density (J_d) is not even 10 percent of J_r. Below this voltage, J_d is even less important. The dominance of J_r is presumably due to defects initially present in the junction region of the cell. The J_r term increases linearly with junction thickness (W_j) and exponentially with the electric field in the junction, E_j. Since $E_j \cong V_j/W_j$, J_r is high for both thick and thin junctions, with an optimum thickness that is between the two.

Figure 1 is characteristic of unirradiated high-quality [18- to 19-percent air mass zero (AM0)] GaAs solar cells. The three current contributions in this semi-log plot add up to the calculated cell current (LIDC) for comparison with the experimental data (LIDX). Beyond the illuminated data, the cell area (8 cm^2), base doping (3 x 10^{23}/m^3), and principal junction defect level (with respect to mid-gap) are included. For simplicity, a trap gap of 0.12 eV is selected to keep the J_r line straight at this stage. The correlation coefficient of 0.99983 is weighted heavily by the higher density of points at high voltages. The apparently poor fit at low voltages results from a nonlinear shunt current which was fitted with a linear term. The actual difference between the data and the model is less than 1 mA (out of an I_{sc} of 251 mA). The current resolution is seen to be approximately ±0.2 mA.

For solar cells that have been irradiated, the contribution of J_r remains greater than that of J_d except near the maximum voltage, where the two terms are approximately equal. Figure 2 is a typical analysis result for electron-irradiated GaAs solar cells. Note that both J_d and J_r have increased so that the relative contributions of the terms are similar to those from the unirradiated cells. For cells from U.S. vendors, this trend continues to at least 10^{16}e$^-$/cm^2. The correlation coefficient and best value for series resistance are nearly unchanged from those of the unirradiated sample; however, the diode current data and calculated shunt current at low voltages have both increased slightly.

Figure 3 shows the effects of proton irradiation on GaAs solar cell current contributions. Two major differences from electron-irradiated cells are seen: the bulk current contribution is now negligible, and the series resistance has increased significantly (from 0.001 to 0.041 Ω). Comparison of electron- and proton-irradiated cells, degraded to the same power, indicates more degradation in J_r (and R_s) and less in J_d from protons. The relative effect on cell characteristics from protons is a lower V_{oc} and higher I_{sc}. Study of these combined effects provides two possible explanations. One is that protons damage junctions more than do electrons, and that they lower the bulk carrier concentration more with less change in carrier lifetime. The second explanation is that the higher reduction in carrier concentration increases the junction field-region thickness (and thereby J_r) and provides a drift field to increase carrier collection (greater effective diffusion length) and I_{sc}.

In Figure 4, the same data as in Figure 3 have been reanalyzed; however, the expression for shunt current has been changed in the model. The modification is based on earlier studies which indicated that most of the observed shunt currents result from a few individual leakage paths through the junction. These paths are shortened as the junction depletion layer collapses under forward bias. Thus, the effective resistance decreases with increasing junction voltage. As a second approximation, a fixed value was maintained for R_{sh}, but $(V - IR_s)^2/R_{sh}$ was substituted for the shunt term in equation 1. The results in Figure 4 are a closer fit to data in the low-voltage region, but provide a lower correlation coefficient than in Figure 3. The other terms are not significantly changed except for J_d, which is at the noise level. This exercise demonstrates that, while the fit can be improved at low voltages, the effect on the critical currents (J_r in this case) is quite small.

Figure 5 is an example of the large differences noted in analyses of Mitsubishi GaAs cells compared to those from U.S. manufacturers. At $10^{16}/cm^2$ 1-MeV electrons, the results appear much closer to the proton results of Figure 3 than to the electron results of Figure 2. The proton irradiation results for the Mitsubishi cells are similar to those from the U.S. cells, but with a higher series resistance (0.27 vs ~0.04 Ω) and higher I_{sc}. The conclusion is that the Mitsubishi cells have lower doping in either (or both) the emitter or base layers. Radiation reduces the carrier concentration further, and the junction field reaches further into the low doped layer(s).

Analysis of GaAs-on-germanium cells (ref. 4) indicates that the principal difference between these cells and GaAs/GaAs is at BOL, where a higher level of junction defects is proposed. With exposure to radiation, the difference in J_r diminishes as radiation-induced defects come to dominate the results. Table I gives typical values for cell characteristics before and after irradiation.

Table I. Results of I-V Analysis on GaAs Solar Cells

Condition	J_d (A/cm^2)	J_r (A/cm^2)	R_s (Ω)
GaAs			
Initial	2×10^{-19}	1×10^{-10}	<0.01
10^{15} e/cm^2	4×10^{-18}	6×10^{-10}	<0.01
10^{16} e/cm^2	4×10^{-17}	2×10^{-9}	<0.01
10^{13} p/cm^2	3×10^{-18}	8×10^{-9}	0.04
GaAs/Ge			
Initial	5×10^{-20}	4×10^{-10}	<0.01
10^{15} e/cm^2	4×10^{-18}	1×10^{-9}	<0.01
10^{16} e/cm^2	5×10^{-17}	2×10^{-9}	<0.01
10^{13} e/cm^2	5×10^{-17}	1×10^{-8}	0.04

The separation of cell I-V curves into junction and bulk contributions, and the differences observed in degradation rates for V_{oc} and I_{sc} from protons and electrons, provide a basis for understanding why a distinction must be made between cell I-V degradation parameters for proton-irradiated solar cells. The greater effect of protons on J_r, relative to that from electrons, increases GaAs solar cell degradation because the J_r term is dominant here, while J_d is dominant in silicon solar cells. The I-V analysis technique provides not only a tool in the design of solar cells for benign and radiation environments, but also a means of studying radiation damage at the defect level.

It can be concluded from this study that J_r dominates nearly all GaAs cells tested, except for unirradiated Mitsubishi cells, which appear to have a different doping profile. Irradiation maintains or increases the dominance by J_r, and proton irradiation increases J_r more than does electron irradiation. The U.S. cells have been optimized for BOL and the Japanese for EOL. I-V analysis indicates ways of improving both the BOL and EOL performance of GaAs solar cells.
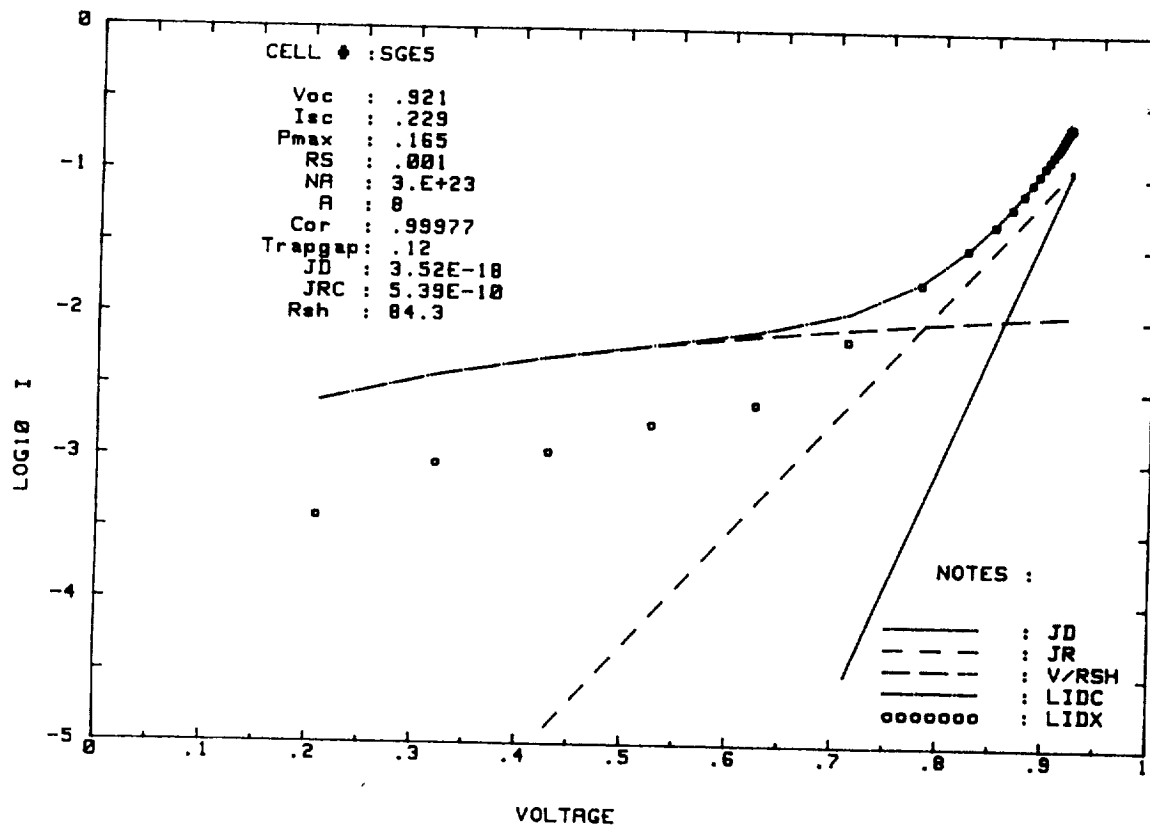
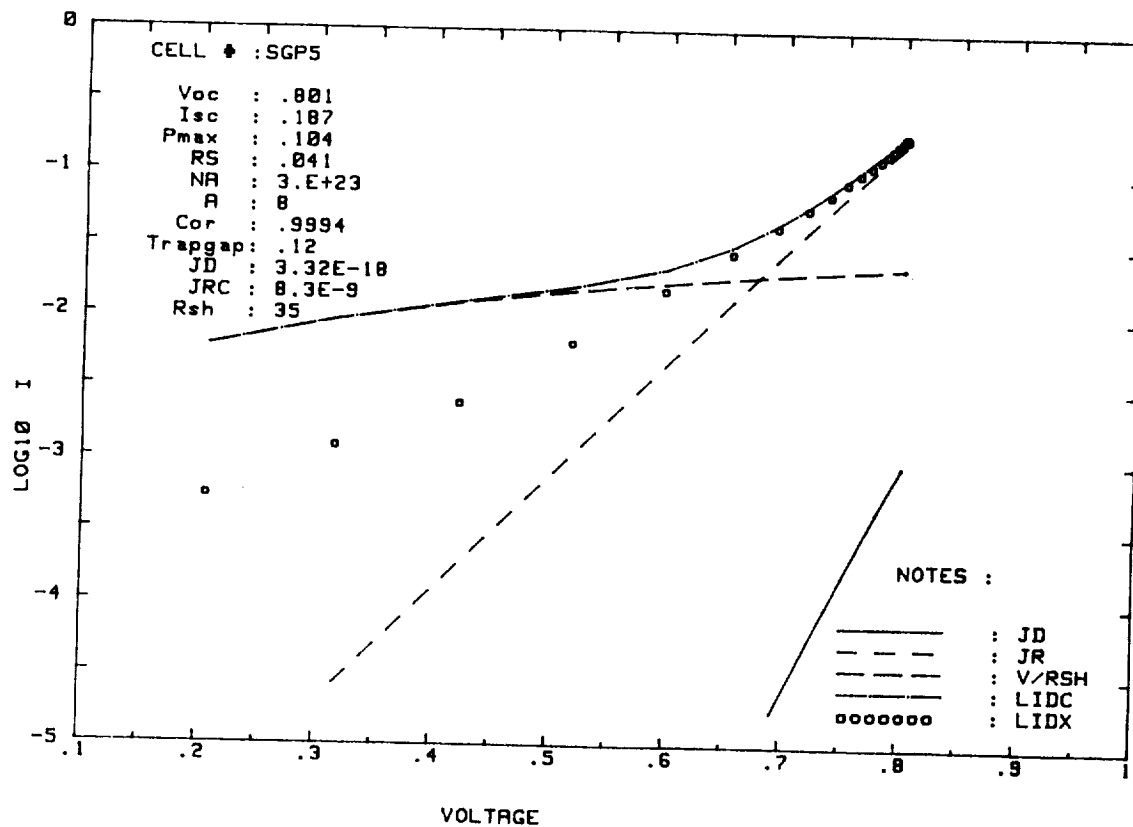Figure 2. Spectrolab GaAs Solar Cell After $10^{15}/cm^2$ 1-MeV Electrons

Figure 3. Spectrolab GaAs Solar Cell After $10^{13}/cm^2$ 10-MeV Protons
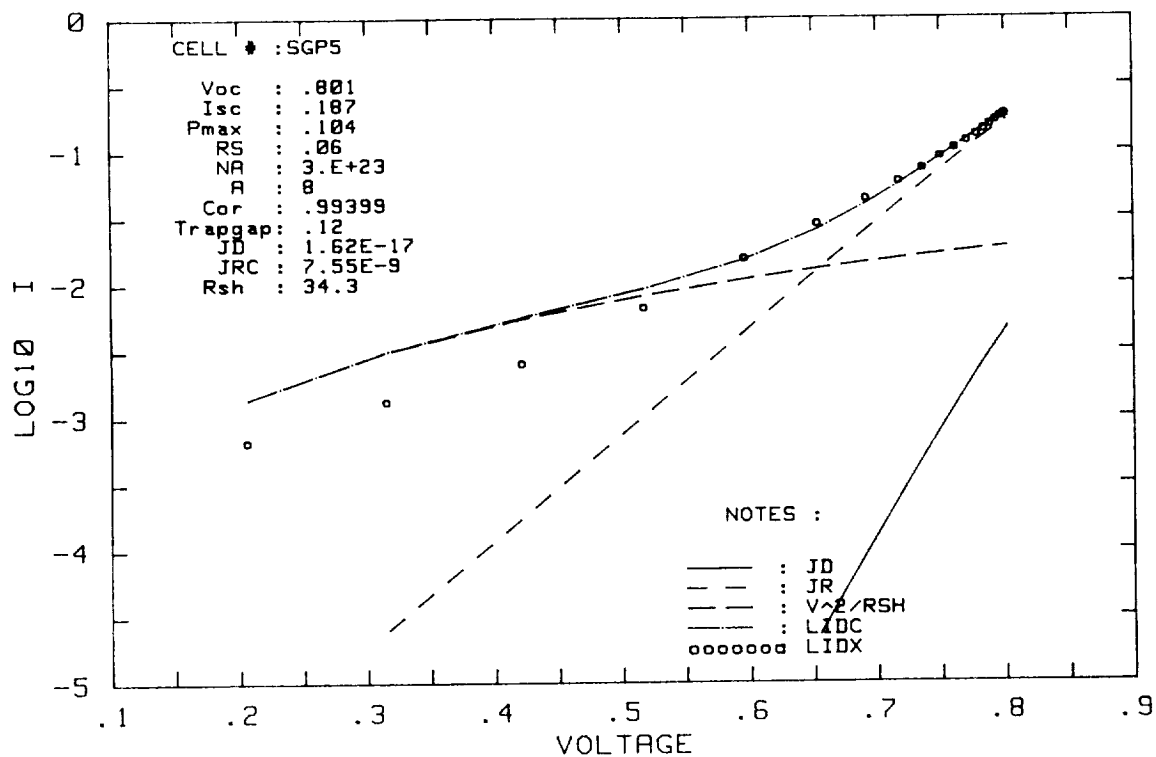
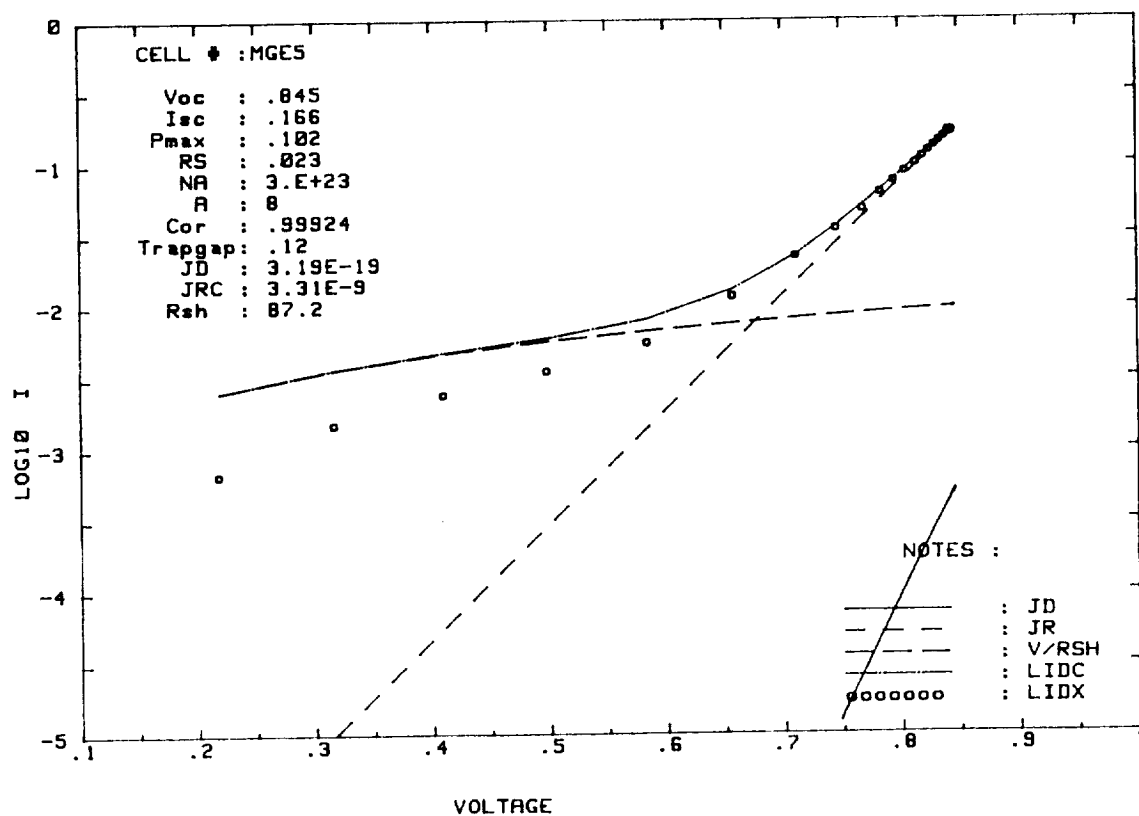Figure 4. Proton-Irradiated Spectrolab Cell With V^2 Dependence In Shunt Term

Figure 5. Mitsubishi GaAs Solar Cell After $10^{16}/cm^2$ 1-MeV Electrons

REFERENCES

1. Rittner, E. S.; Meulenberg, A.; and Allison, J. F.: "Dependence of Efficiency of Shallow Junction Silicon Solar Cells on Substrate Doping," *Journal of Energy*, Vol. 5, No. 1, January–February 1981, pp. 9–14. [See also: Rittner, E. S, "An Improved Theory for the Si p-n Junction Solar Cell," *Journal of Energy*, Vol. 1, No. 1, January–February 1977, pp. 9–17.]

2. Meulenberg, A., Jr.: "Developments Toward an 18% Efficient Silicon Solar Cell," Final Report for Contract NAS-3-22217, NASA CR 168141, April 1983.

3. Meulenberg, A.: "Evidence for a Permanent Single-Event Upset Mechanism," *IEEE Transactions on Nuclear Science*, Vol. NS-31, No. 6, December 1984, pp.1280–1283.

4. Meulenberg, A.; and Rittner, E. S.: "Limiting Processes in Shallow Junction Solar Cells," 3rd Solar Cell High Efficiency and Radiation Damage Meeting, NASA Lewis Research Center, June 1979.

5. Herbert, G. A., *et al.*: "Electron and Proton Displacement Damage in Production Line Quality Silicon and Gallium Arsenide Solar Cells," 4th International Photovoltaic Science and Engineering Conference, Sydney, Australia, February 1989.

6. Maurer, R. H., *et al.*: "Gallium Arsenide Solar Cell Radiation Damage Study," *IEEE Transactions on Nuclear Science*, Vol. NS-36, No. 6, December 1989, pp. 2083–2091. (See also these *Proceedings*.)
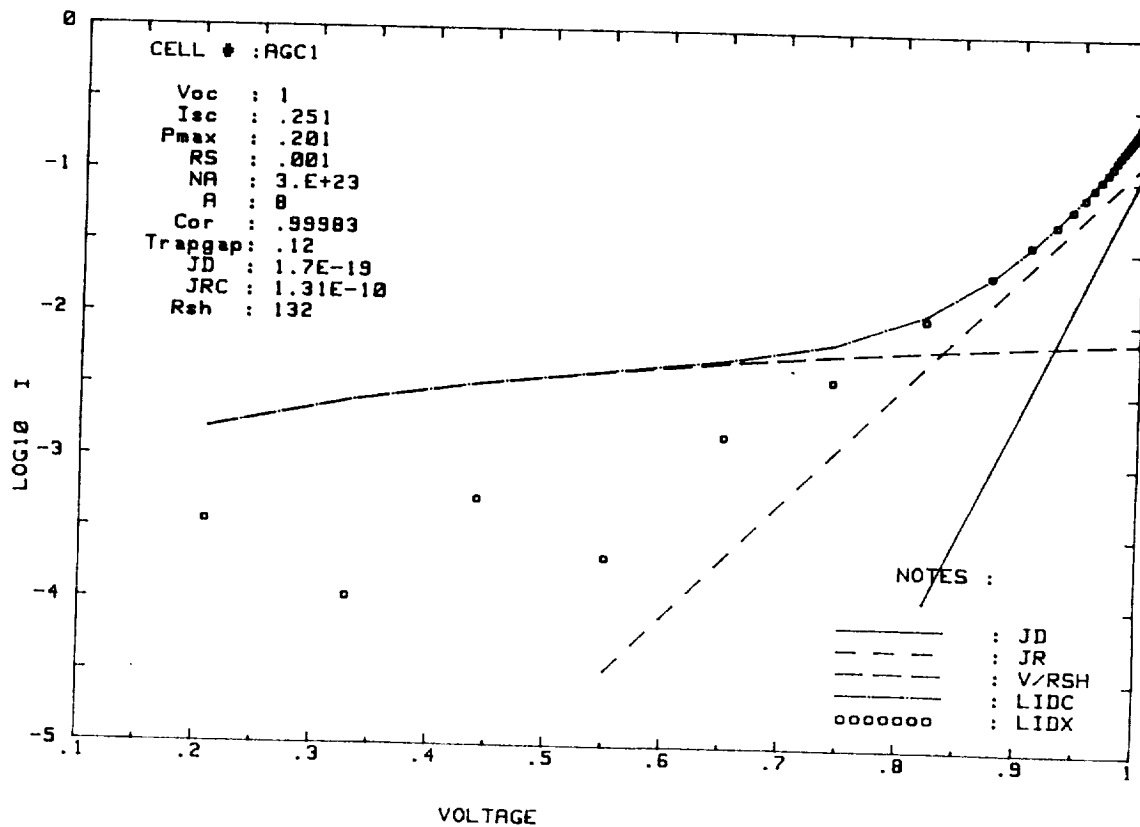
Figure 1. Unirradiated ASEC GaAs Solar Cell